Combinatorial Vector Field Topology in 3 Dimensions

Wieland Reich, Dominic Schneider, Christian Heine, Alexander Wiebel,
Guoning Chen, Gerik Scheuermann

Abstract In this paper, we present two combinatorial methods to process 3-D steady vector fields, which both use graph algorithms to extract features from the underlying vector field. Combinatorial approaches are known to be less sensitive to noise than extracting individual trajectories. Both of the methods are a straightforward extension of an existing 2-D technique to 3-D fields. We observed that the first technique can generate overly coarse results and therefore we present a second method that works using the same concepts but produces more detailed results. We evaluate our method on a CFD-simulation of a gas furnace chamber. Finally, we discuss several possibilities for categorizing the invariant sets respective to the flow.

1 Introduction

Topology-based methods are of increasing importance in the analysis and visualization of datasets from a wide variety of scientific domains such as biology, physics,

Wieland Reich
University of Leipzig, e-mail: reich@informatik.uni-leipzig.de

Dominic Schneider
Universtity of Leipzig, e-mail: schneider@informatik.uni-leipzig.de

Christian Heine
University of Leipzig, e-mail: heine@informatik.uni-leipzig.de

Alexander Wiebel
Max-Planck-Institut for Human Cognitive and Brian Sciences, Leipzig, e-mail: wiebel@cbs.mpg.de

Guoning Chen
University of Utah, e-mail: chengu@sci.utah.edu

Gerik Scheuermann
University of Leipzig, e-mail: scheuermann@informatik.uni-leipzig.de

engineering, and medicine. Especially in the context of vector fields great research efforts have been undertaken to segment the domains of the available data into meaningful regions. In particular, steady vector field topology tries to find regions in which streamlines exhibit similar behavior. These regions can be used for further processing and analysis of the vector field itself or to simplify the visualization. The latter is usually achieved by drawing only the region's borders, the so called separatrices. This produces less geometry and thus less visual clutter than illustrating all particulars of the field. Both of these advantages are relevant for two-dimensional vector fields, but become critical for three-dimensional vector fields where possible occlusion appears as additional problem.

Different methods for vector field topology in two as well as in three dimensions have been proposed in the past. The most recent advances come from the sub-field of combinatorial vector field topology. Unfortunately, up to now only techniques for two-dimensional fields have been presented in this context so far. In this paper we try to fill the gap of missing combinatorial vector field topology methods for three dimensions. We present two methods to process three-dimensional fluid flows, which both use graph algorithms to extract features from the underlying vector field. We will apply the methods to several synthetic data sets and one of them to a CFD-simulation of a gas furnace chamber. In the end, we provide several options for categorizing the invariant sets respective to the flow.

2 Related Work

In the history of flow visualization – a survey can be found in [27] and [28] – topological methods make their steady appearance. Helman and Hesselink [11] introduced them to the visualization community starting with extracting and classifying singularities also known as critical points. Many other topological structures beyond singularities have been used in visualization. Periodic orbits have been subject to visualizations by Theisel *et al.* [15] and Wischgoll and Scheuermann [17]. Peikert and Sadlo [13] improved the display of invariant manifolds for saddle points and periodic orbits. Displaying all such invariant manifolds at once leads to an occlusion problem. A solution is to only display their intersection curves, the so-called saddle connectors [16]. Tricoche *et al.* [18] proposed vector field simplification based on topological methods. In the recent past Morse theory has gained interest in the analysis of vecter field data. Zhang *et al.* [31] and Chen *et al.* [1] introduced Morse decomposition and Conley index theory to the visualization comunity. Edelsbrunner *et al.* [19] and Guylassy *et al.* [20] use Morse-Smale complexes to process the gradient field obtained from scalar data. Reininghaus and Hotz [21] process 2-D vector fields with a method based on Forman's work [25]. Unlike our method, it transforms the cells and simplices of lower dimension, i.e. edges and vertices, directly into a graph. In contrast, our work is the extension of Morse decompositions of flows on 2-dimensional manifolds, which has been subject of the work of Chen *et al.* [1, 2], to 3 dimensions. An example visualization obtained with [1] is given in Fig. 1.

3 Vector Fields, Flows, and Morse Decompositions

Let $X' = F(X)$ be a differential equation defined on $\mathbb{R}^3$, then the associated flow is a continuous function $\Phi : \mathbb{R} \times \mathbb{R}^3 \to \mathbb{R}^3$, satisfying

$$\Phi(0,x) = x, \tag{1}$$

$$\Phi(t_1, \Phi(t_2,x)) = \Phi(t_1 + t_2, x). \tag{2}$$

It holds

$$\frac{d}{dt}\Phi(t,x)_{|x_0} = F(x_0). \tag{3}$$

$S \subset \mathbb{R}^3$ is an **invariant set** if $\Phi(t,S) = S$ for all $t \in \mathbb{R}$. For example, the trajectory of any point $x \in \mathbb{R}^3$ is an invariant set.

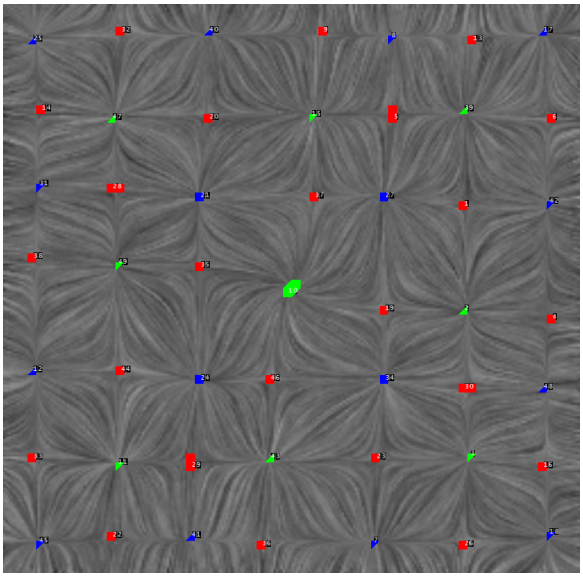

(a) A vector field visualized with a Line Integral Convolution. Extracted Morse sets are displayed as green (source), red (saddle), or blue (sink).

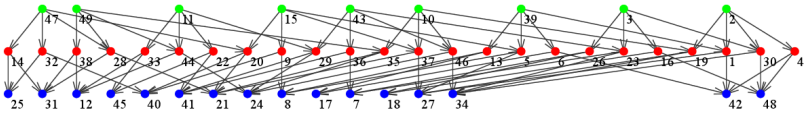

(b) The resulting Morse connection graph. The nodes have the same color as the represented fixed points in the field above.

Fig. 1 A Morse decomposition of a planar field computed with the algorithm by Chen *et al.* [1].

A compact set $N \subset \mathbb{R}^3$ is called **isolating neighborhood** if the maximal invariant set S, that is contained in N, lies in the interior of N. A set S is an **isolated invariant set**, if there exists an isolating neighborhood N so that S is the maximal invariant set contained in N.

Hyperbolic fixed points and periodic orbits are examples of isolated invariant sets, but also the space of their connecting trajectories. Let $\varepsilon > 0$ be small, we define the **exit set** of an isolating neighborhood as

$$L = \{x \in \partial N \mid \Phi((0,\varepsilon),x) \cap N = \emptyset\} \tag{4}$$

The so called index pair (N,L) will be of further interest in Sec. 6, when we classify isolated invariant sets.

The **alpha-** and **omega limit sets** of $x \in \mathbb{R}^3$ are

$$\alpha(x) = \bigcap_{t<0} cl(\Phi((-\infty,t),x)),\ \omega(x) = \bigcap_{t>0} cl(\Phi((t,\infty),x)) \tag{5}$$

where cl denotes the closure of a set.

A **Morse decomposition** $\mathscr{M}$ of $X \subset \mathbb{R}^3$ is a finite collection of isolated invariant subsets of X, called **Morse sets** M:

$$\mathscr{M}(X) = \{M(p) \mid p \in \mathscr{P}\}, \tag{6}$$

such that if $x \in X$, then there exists $p,q \in \mathscr{P}$ such that $\alpha(x) \subset M(q)$ and $\omega(x) \subset M(p)$. In addition, there exist a partial order $>$ on $\mathscr{P}$ satisfying $q > p$ if there is an $x \in X$ such that $\alpha(x) \subset M(q)$ and $\omega(x) \subset M(p)$.

4 Geometry-Based Flow Combinatorialization

In this section we present an algorithm that computes regions with source, saddle, and sink-like behavior and the Morse connection graph between these regions, for a vector field defined on a simplicial 3-D mesh $\mathbf{T} = \bigcup T_i$.

We start by defining an equivalence relation between tetrahedra: $T_i \sim T_j$ if and only if there exists a sequence of connected tetrahedra $T_i,\ldots,T_j$ where all intermediate faces are non-transversal, i.e. flow through the face is not uni-directional. Each face can be easily checked by testing whether the flow vector at each of its 3 vertices produces the same sign when the inner product with the face normal is computed. For this procedure we use linear interpolation on the tetrahedral mesh. The resulting equivalence relation partitions the domain into polyhedral regions $\mathbf{R} = \bigcup R_i$, with all faces being transversal.

Then we construct a *flow graph*, which encodes a combinatorial description of the flow in the field. In this graph, each equivalence class of cells R_i is represented by a node u_i. If there exists a common face between two elements R_i and R_j of $\mathbf{R}$ and the flow points from R_i to R_j, we add an arc (u_i,u_j) in the graph.

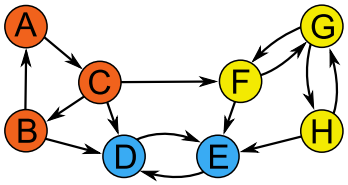

Fig. 2 A drawing of strongly connected components. Different colors describe the pairwise disjoint sets of nodes in this graph, in each existing a path from an arbitrarily chosen node to all others of the same component.

We then compute the flow graph's strongly connected components using the popular algorithm by Tarjan [9]. A strongly connected component of a graph is a maximal subgraph in which for each pair of vertices u_i, u_j there exists a directed path from u_i to u_j. An example is given in Fig. 2. Strongly connected components describe regions of recurrent flow. As the strongly connected components induce an equivalence relation between graph nodes, we compute the quotient graph by adding one node v_i for each strongly connected component c_i and an arc from nodes v_i to v_j if there is an arc from any node of c_i to any node of c_j. It is trivial to show that the quotient graph on the strongly connected components of a graph is an acyclic directed graph.

From the quotient graph we then remove all nodes that neither are sources or sinks nor contain a critical point with respect to vector field topology. The removed nodes represent trivial flow behavior, e.g. all entries in the Conley index are zero. The Conley index is a topological invariant discussed in Sec. 6. To preserve connectivity, we add an arc for each combination of the removed node's successors with its predecessors. The resulting graph's nodes represent regions which contain isolated invariant sets. A proof that the resulting graph, which we henceforth call Morse connection graph (MCG), encodes a Morse decomposition of the phase space was given in [4]. We classify each node, which represents a Morse set, according to Sec. 6. We then show the graph in an additional window using the algorithm by Gansner *et al.* [30] for graph layout. We restrict all sources and all sinks to be on one layer, respectively. Furthermore we remove all transitive arcs, i.e. arcs (v_i, v_j) for which there exists a path from v_i to v_j not using (v_i, v_j), as they complicate graph layout but do not improve perception ([29], Chapter 1).

This algorithm works well with regions in vector fields with gradient-like flow behavior (Fig. 3). For highly rotational fields, the purely geometry-based method can separate only few regions. Theoretically, one could try to find a new tetrahedralization of the trajectory space, where all cells have transverse faces, i.e. unidirectional flow everywhere. This is a complicated task and instead we turn our attention to a streamline-based approach.

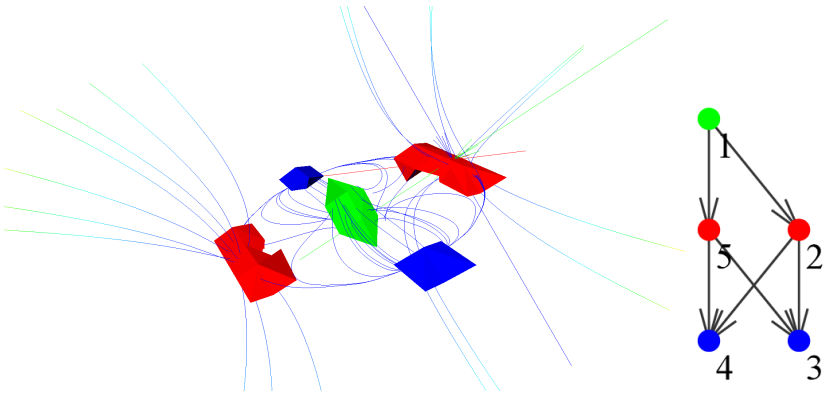

(a) Morse sets in a vector field

(b) Morse connection graph

Fig. 3 A decomposition with the geometry-based algorithm of 3-D data containing two sinks (blue), a source (green), and two saddles (red).

5 Streamline-Based Flow Combinatorialization

An improvement of the geometry-based Morse decomposition was explained in [2]: For each cell a set of streamlines is seeded uniformly across the cell's volume and integrated for a short time or length and the cells in which the streamlines end are recorded. A mathematical foundation, that this is leading to Morse decomposition of the phase space, is given in [5].

Having a tetrahedron T_1 in a mesh $\mathbf{T}$, then there exists a union of tetrahedra T_i, so that the image of T_1 under streamline integration lies completely in $\bigcup T_i$. We will refer to it as an outer approximation (Fig. 4). The resulting combinatorial multi-valued map $\mathscr{F}$:$\mathbf{T}\rightarrow\mathbf{T}$ is then encoded into the flow graph. We then proceed in the same way as geometry-based method, computing strongly connected components, quotient graph, and removing cells with trivial flow behavior.

Once the graph is created, we cannot influence the outcome anymore, so let us discuss the modalities of the integration. We used DoPri5 [24] and decided to integrate all tetrahedra by a fixed arc-length. The reason is simple, some cells in slowly moving regions will not have moved at all, while others may have reached the boundary. Furthermore, there are two possibilities to reconstruct the integration image, both using a sampling of the cell, so dense, that eventually no image cell will slip through the net. Using FTLE [23] or a similar predictor that just integrates the vertices to compute the stretching of the cell is not rigorous. Though, we could get adequate results with that. A more rigorous, but computationally costly method is to integrate the uniformly distributed seeding points stepwise for small times and adaptively place new streamlines between them like in Hultquist's algorithm for stream surfaces [12]. Placing seeding points just on the boundary of the cell is an option,

but does not spare much of the computation time, since the whole volume must be reconstructed after the integration.

After computing the images of all seeding points, we collect their cell indices. Taking all of the neighbors of all computed image cells into the outer approximation is possible, but will lead to coarse results. More rigorous enclosing techniques are discussed in [7].

6 Identification of Morse Sets

Finally, this algorithm is sensitive to the parameter of the integration length. Integrating for a too small arc-length will lead to many so called false positives, where highly spiraling flow does not differ from closed streamlines. In Fig. 5 we applied the algorithm to a segment of a gas furnace chamber. We were able to find one closed streamline which was close together with a fixed point in the same Morse set. This reveals a weakness of our combinatorial algorithm: If the closed streamline is very small, then its outer approximation will topologically be a ball, not a torus. On the other hand, the questions arises, whether a refinement is really necessary in all cases. The grade of simplification can be controlled by the arc-length-parameter and topological invariants are able to categorize a Morse set that consist of multiple fixed points and periodic orbits.

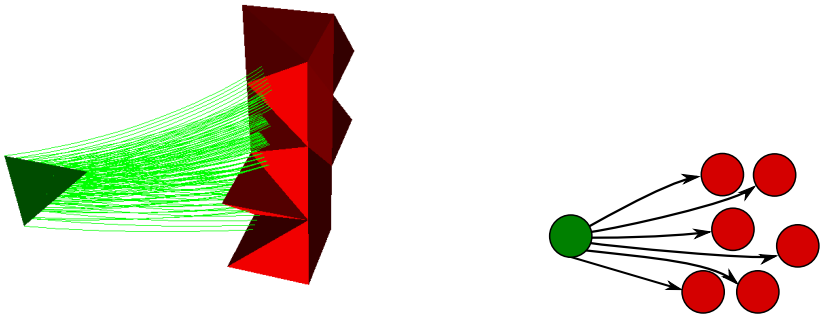

(a) A union of cells (red) that encloses the image of the green cell under streamline integration.

(b) The multi-valued map is encoded into a graph.

Fig. 4 Outer approximation.

6.1 Classical Methods

For fixed points of first order, a commonly used method is the evaluation of the eigenvalues of the Jacobi matrix at the corresponding position. For a hyperbolic closed streamline, a Poincaré section plane can be used ([10]). As we have no guarantee that these structures are always isolated from each other in our obtained Morse sets, we are not going to apply them.

6.2 Graph Analysis

A very simple, but coarse way to identify a Morse set is to enumerate the connected arcs before the node cancellation in the Morse connection graph. If all of the arcs

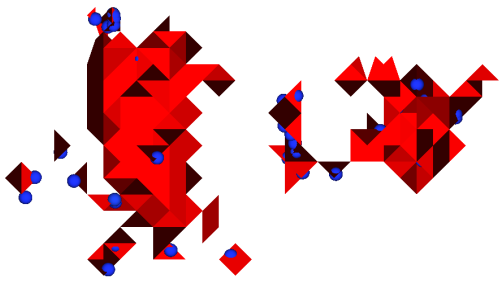

(a) blue: spheres indicating saddle points, red: extracted Morse sets

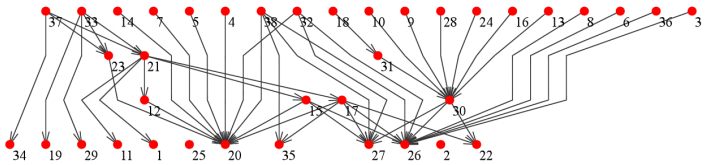

(b) As we expected, there are only saddle-like Morse sets in divergence free CFD-simulations, so we aligned the graph layout, that they are not displayed on a single line like in Fig. 1.

Fig. 5 A segment of a gas furnace chamber processed with the streamline-based Morse decomposition. The geometry-based algorithm was only able to extract one(!) Morse set in this highly turbulent flow.

are outgoing, it is a source. Analogous, if all arcs are incoming, it is a sink. If arcs of mixed types exist, it is a saddle-like Morse set. Eventually no more conclusions of the nature about the Morse set are possible.

6.3 Poincaré Index

The Poincaré index is a topological invariant as well. It is strongly related to the Conley index, but does not contain as much information. However, it has been successfully used to simplify vector field topology in 2 and 3 dimensions. It also can deal with fixed points of higher order [18].

6.4 Conley Index

A far more accurate topological invariant is the Conley index, which was introduced to the visualization community by Chen *et al.* [1], based on the comprehensive theoretical work by Mischaikow [3]. In [1] and [2], Morse decompositions and a method of computing the Conley index in two dimensions are explained and a number of important indices were illustrated, i.e. those of hyperbolic fixed points and closed streamlines.

Let N be an isolating neighborhood and L its exit set as they were defined in Sec. 3.

Definition 1. The (homological) **Conley index** is defined as

$$CH_*(N) = H_*(N/L),$$

where $H_*(N,L)$ is the relative homology of the index pair (N,L).

Since all $CH_i(N)$ can be arbitrary finite generated Abelian groups, a complete classification of all possible Conley indices is impossible. Important ones are

Conley index	flow is equivalent to
$CH_*(x) = (\mathbb{Z},\ \{0\},\ \{0\},\ \{0\})$	attracting fixed point
$CH_*(x) = (\{0\},\ \mathbb{Z},\ \{0\},\ \{0\})$	fixed point with one-dimensional unstable manifold
$CH_*(x) = (\{0\},\ \{0\},\ \mathbb{Z},\ \{0\})$	fixed point with two-dimensional unstable manifold
$CH_*(x) = (\{0\},\ \{0\},\ \{0\},\ \mathbb{Z})$	repelling fixed point
$CH_*(\Gamma) = (\mathbb{Z},\ \mathbb{Z},\ \{0\},\ \{0\})$	attracting closed streamline
$CH_*(\Gamma) = (\{0\},\ \mathbb{Z},\ \mathbb{Z},\ \{0\})$	saddle-like closed streamline
$CH_*(\Gamma) = (\{0\},\ \mathbb{Z}_2,\ \mathbb{Z}_2,\ \{0\})$	twisted saddle-like closed streamline
$CH_*(\Gamma) = (\{0\},\ \{0\},\ \mathbb{Z},\ \mathbb{Z})$	repelling closed streamline
$CH_*(\emptyset) = (\{0\},\ \{0\},\{0\},\ \{0\})$	empty set

The rank of $CH_i(N)$ is called the i-th Betti number. In particular the Poincaré index is the alternating sum of the Betti numbers:

$$index(N) = |(CH_0(N))| - |(CH_1(N))| + |(CH_2(N))| - |(CH_3(N))| \tag{7}$$

It should be noted, that a non-trivial Conley index does not guarantee the presence of the corresponding isolated invariant set, but it indicates, that flow inside the isolating neighborhood is equivalent to it. Similarly, a trivial Conley index, which means that all groups are identical $\{0\}$, could just mean, that the included invariant sets are cancelling each other out.

A nontrivial Conley index always implicates the existence of at least one isolated invariant set inside the isolating neighborhood. This statement is also known as the **Wazewski property**.

Readers who would like to know more about the computation of homology are referred to [3] and [6]. Readers who are not familiar with homology may also have a look at [26]. Efficient implementations of homology algorithms already exist [8], so we do not need to concern about these issues.

Recent publications ([13] an [14]) have particulary shown interest in visualizing closed streamlines of saddle-like behavior. Fig. 6 shows, that our algorithm is able to extract an artificially generated one. Peikert *et al.* were able to find a twisted saddle-like closed streamline from a CFD simulation of a Pelton turbine.

To the best of our knowledge, not much is explored about the extraction of compact invariant 2-manifolds from fluid flows, e.g. on an invariant torus (subject of publication [22]) almost every case from gradient-like flow to chaotic behavior may exist. We cannot describe chaos with a topological invariant.

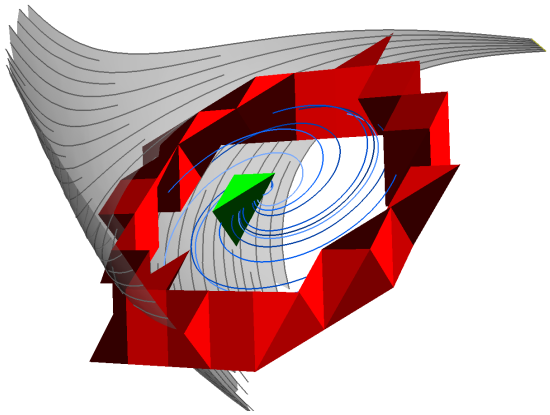

Fig. 6 A saddle-like closed streamline extracted by the streamline-based Morse decomposition. Such a feature cannot be found be arbitrarily placed individual streamlines [17]. The stream surface (grey) indicates a divergent behavior. But inside the stable manifold, which is a plane, where the blue trajectories are placed, it is also connected with a fixed point that is a source. So the extracted Morse set of red tetrahedra must act as a saddle.

7 Results

We applied both techniques from Sec. 4 and Sec. 5 to several artificially generated data and CFD-simulation datasets, Fig. 3,Fig. 5 and Fig. 6 are just a selection.

Where the results of the geometry-based Morse decomposition become more coarse when the curl of the field increases, the streamline-based version can compensate this problem partially by raising the maximum arclength of integration. This will lead to a higher computation time, of course. It seems like that there exists a ideal integration range for each field, because the extracted structures cannot become thinner than the diameter of a cell.

A gas furnace chamber (Fig. 5) poses a real challenge due to highly turbulent flow and is recorded by the following table. All computations were done by a single core cpu with 2.4 GHz:

cells	arclength of integration	time to process	Morse Sets	number of arcs in the MCG
31881	5	490s	31	104
31881	10	1136s	36	107
31881	15	1767s	38	87

8 Conclusions and Future Work

We have shown 2 approaches to a Morse decomposition in 3 dimensions and different possibilities to classify the obtained Morse sets. We found out in our experiments, that for a large fixed integration length, there are still Morse sets remaining, that cannot be further decomposed, so there is plenty of potential in improving the streamline-based algorithm, i.e. repeatedly applying it to the remaining sets with increasing arc-length parameter. In addition, a parallelization must be considered as a must in future work. The main difference to classical topology is, that the equivalence classes of streamlines are not induced by having the same ω- and α- limit set by integration, but being in the same strongly connected component. Though the complex shape of Morse sets has theoretically a higher variation in 3 dimensions, practically fixed points of saddle character will dominate in data obtained from CFD-Simulations. The clusters of cells do not always give an immediate insight into the behaviour of the field, but it still can be used as a preprocessing algorithm for finer techniques. An interesting challenge in the future is to make general conclusions in how exactly the size of the grid and the length of integration will inflict the results.

Acknowledgements We want to thank Tomasz Kaczynski, Matthias Schwarz, the people from the Krakau research group for “Computer Assisted Proofs in Dynamics” and the reviewers for many valueable hints and comments.

References

1. G. Chen , K. Mischakow, R.S.Laramee, P. Pilarczyk, "Vector Field Editing and Periodic Orbit Extraction Using Morse Decomposition", *IEEE Transactions on Visualization and Computer Graphics*, Vol. 13, 769-785, 2007.
2. G. Chen , K. Mischakow, R.S.Laramee, "Efficient Morse Decompositions of Vector Fields", *IEEE Transactions on Visualization and Computer Graphics*, Vol. 14, 848-862, 2008.
3. K. Mischaikow, "The Conley Index Theory: A Brief Introduction", *Banach Center publications*, Vol. 47, 1999.
4. E. Boczko, W. Kalies, K. Mischaikow, "Polygonal Approximation of Flows", *Topology and its Applications*, Vol. 154, 2501-2520, 2007.
5. W. Kalies and H. Ban, "A Computational Approach to Conley's Decomposition Theorem", *J. Computational and Non-Linear Dynamics*, Vol. 1, No. 4, 312-319, 2006.
6. T. Kaczynski, K. Mischaikow, M. Mrozek, *Computational Homology*, Springer, 2003.
7. M. Mrozek, P. Zgliczynski, "Set arithmetic and the enclosing problem in dynamics", *Annales Polonici Mathematici*, 237-259, 2000.
8. *Computer Assisted Proofs in Dynamics group*
http://capd.ii.uj.edu.pl
9. R. Tarjan, "Depth-first search and linear graph algorithms", *SIAM Journal of Computing*, Vol. 1, 146-160, 1972.
10. M. Hirsch, S. Smale, R. Devaney, *Differential Equations, Dynamical Systems and An Introduction to Chaos*, Elsevier, 2004.
11. J. Helman, L. Hesselink, "Visualizing Vector Field Topology in Fluid Flows", *IEEE Computer Graphics and Applications*, Vol. 11, 36-46, 1991.
12. J. Hultquist, "Constructing Stream Surfaces in Steady 3-D Vector Fields", *Proceedings IEEE Visualization 1992*,171-178, 1992.
13. R. Peikert, F. Sadlo, "Topologically Relevant Stream Surfaces for Flow Visualization", *Proc. Spring Conference on Computer Graphics*,171-178, 2009.
14. R. Peikert, F. Sadlo, Flow Topology Beyond Skeletons: Visualization of Features in Recirculating Flow, *Topology-Based Methods in Visualization II*, Springer, 145-160, 2008.
15. H. Theisel, T. Weinkauf, H. Hege, H. Seidel, "Grid Independent Detection of Closed Streamlines in 2D Vector Fields", *Proc. Vision, Modeling, and Visualization 04*, 2004.
16. H. Theisel and T. Weinkauf and H.-C. Hege and H.-P. Seidel, Saddle Connectors - An Approach to Visualizing the Topological Skeleton of Complex 3D Vector Fields, *Visualization Conference, IEEE*, 0,30, 2003.
17. T. Wischgoll, G. Scheuermann, "Detection and Visualization of Planar Closed Streamlines", *IEEE Trans. Visualization and CG*, Vol. 7, 165-172, 2001.
18. X. Tricoche, G. Scheuermann, H. Hagen, "A Topology Simplification Method for 2D Vector Fields", *IEEE Visualization 00 Proc.*, 359- 366, 2000.
19. H. Edelsbrunner, J. Harer, A. Zomorodian, "Hierarchical morse complexes for piecewise linear 2-manifolds", *Proc. of the seventeenth annual symposium on Computational Geometry*, 70-79, 2001.
20. A. Guylassy, P. Bremer, B. Hamann, V. Pascucci, "A practical approach to morse-smale complexes for three dimensional scalar functions", *IEEE Transactions on Visualization and Computer Graphics*, 1619-1626, 2008.
21. J. Reininghaus, I. Hotz, "Combinatorial 2D Vector Field Topology Extraction and Simplification", *Topology in Visualization*, 2010.
22. A. Sanderson, G. Chen, X. Tricoche, D. Pugmire, S. Kruger, J. Breslau, "Analysis of Recurrent Patterns in Toroidal Magnetic Fields", *IEEE Trans. Visualization and CG*, Vol. 16, 1431-1440.
23. G. Haller, "Distinguished Material Surfaces and Coherent Structures in Three-Dimensional Flows", Vol. 149, 248-277, 2001.
24. E. Hairer, P. Syvert, G. Wanner, *Solving ordinary differential equations I: Nonstiff problems*, Springer, 2008.

25. R. Forman, “Combinatorial vector fields and dynamical systems”, *Mathematische Zeitschrift*, Vol. 228, 629-681, 1998.
26. A. Hatcher, *Algebraic Topology* , Cambridge University Press, 2002.
27. F. Post, B. Vrolijk, H. Hauser, R.S. Laramee, H. Doleisch, “The State of Art in Flow Visualization: Feature extraction and Tracking”, *Computer Graphics Forum*, Vol. 22, No. 4, 775-792, 2003.
28. D. Weiskopf, B. Erlebacher, “Overview of Flow Visualization”, *The Visualization Handbook*, 261-278, Elsevier, 2005.
29. G.Di Battista, P. Eades, R. Tamassia, I.G. Tollis, *Graph Drawing*, Prentice Hall, 1999.
30. E.R. Gansner, E. Koutsofios, S.C. North, K.-P. Vo, “A Technique for Drawing Directed Graphs”, *IEEE Trans. Software Eng.*, Vol. 19, No. 3, 214-230, 1993.
31. E. Zhang and K. Mischaikow and G. Turk, Vector Field Design on Surfaces, *ACM Transactions on Graphics*, 25, 2006.